RAA 2020 Vol. **20** No. **7**, 108(11pp) doi: 10.1088/1674–4527/20/7/108

http://www.raa-journal.org *http://iopscience.iop.org/raa*

Research in Astronomy and Astrophysics

Analysis of the X-ray emission from OB stars III: low-resolution spectra of OB stars

Elizaveta Ryspaeva[1,2] and Alexander Kholtygin[2,3]

[1] Crimean Astrophysical Observatory, Nauchny, Crimea 298409, Russia; *e.ryspaeva@yandex.ru*
[2] Saint-Petersburg State University, Saint-Petersburg 198504, Russia; *afkholtygin@gmail.com*
[3] Institute of Astronomy, Russian Academy of Sciences, ul. Pyatniskaya 48, Moscow 119017, Russia

Received 2019 July 21; accepted 2019 December 13

Abstract This paper is the third in our series of papers devoted to the investigation of X-ray emission from OB stars. In our two previous papers, we study the high-resolution X-ray spectra of 32 O stars and 25 B stars to investigate the correlations between the properties of X-ray emission and stellar parameters. We checked if the X-ray hardness and post-shock plasma temperature grow with increasing stellar magnetic field, mass loss rate and terminal wind velocity. Our previous analysis of high-resolution spectra showed that the correlations are weak or even absent. In the present paper, we analyzed low-resolution X-ray spectra, using model-independent X-ray hardness values for checking the above mentioned dependencies. We establish that X-ray luminosities $L_{\rm X}$ weakly depend on the stellar magnetic field. At the same time, $L_{\rm X} \propto \dot{M}^{0.5}$ and $L_{\rm X} \propto E_{\rm kin}^{0.5}$, where $\dot{M}$ is the mass loss rate and $E_{\rm kin}$ is the kinetic energy of the wind. The X-ray luminosities decrease with growing magnetic confinement parameter η. We also argue that there is an additional (probably non-thermal) component contributed to the stellar X-ray emission.

Key words: stars: early-type — stars: spectra: X-Ray

1 INTRODUCTION

The Magnetically Confined Wind Shock model (MCWS, Babel & Montmerle 1997; ud-Doula & Owocki 2002) is one of the basic theories explaining the origin of X-ray emission from OB stars. In two previous papers by Ryspaeva & Kholtygin (2018, 2019), hereafter Paper I and Paper II respectively, we proposed possible consequences from the model. According to our assumptions, the hardness of X-ray spectra increases with enhancing terminal wind velocity, mass loss rate, magnetic field strength and hot plasma temperature. In Paper I and II, these correlations were checked by considering high resolution X-ray spectra of 32 O stars and 25 B stars. We identified lines in the spectra of studied objects and estimated hardness value as a ratio of the highest intensities in lines of adjacent ions.

However, such an approach appeared to be strongly dependent on the procedures of ion selection and line identification. So, it is difficult to test the correlation between spectral hardness and stellar parameters using high resolution spectra. Therefore, in the current paper, low resolution X-ray spectra of OB stars were examined for checking the above mentioned suppositions. For doing this, we evaluated stellar parameters such as plasma temperature and spectral hardness for OB stars. The latter were calculated as a ratio of integral fluxes in the hard spectral range (with photon energy more than 2 keV) and in the soft one (with photon energy below 2 keV).

The present article is organized as follows. The observations and data reduction are described in Section 2. The procedure of spectral modeling is provided in Section 3. The regression analysis of correlations between X-ray emission characteristics and stellar parameters 1is presented and discussed in Section 4. Finally, Section 5 contains general conclusions.

2 OBSERVATIONS AND DATA REDUCTION

The X-ray observations of 93 OB stars obtained by the *XMM-Newton* space observatory in 2001–2017 were analyzed. The list of these stars together with their parameters and the corresponding references is given in Table 1. The distances to these stars are calculated by parallaxes, which are referenced from the SIMBAD database[1]. These parallaxes are available in the Gaia DR2 online catalogue (2018)[2] or in the Hipparcos parallaxes (van Leeuwen 2007; Perryman et al. 1997). Distance to the star HD 93129 is taken from Gagné et al. (2011). Table 2 contains a log of the observations. Some of these objects were studied by us previously in Papers I and II utilizing high resolution X-ray spectra obtained with the Reflecting Grating Spectrometer (RGS). In the present paper, we employed data obtained by the European Photon Imaging Camera (EPIC) on board the *XMM-Newton* satellite. The data reduction was made by SAS 17.0 software following the recommendation of the SAS team[3].

Firstly, we made the preliminary pipeline of observation data files by the *emproc* script for EPIC-MOS1 and EPIC-MOS2 data, and by the *epproc* script for EPIC-PN data. Filtering the EPIC-images from background flares was performed applying the *tabgtigen* and *esfilter* tasks. The stellar spectra were extracted from the filtered images by the *evselect*, *arfgen* and *rmfgen* tasks. The source spectra were obtained from the circular region with radius not smaller than 15′ centered on the stellar coordinates. They were taken from SIMBAD and corrected by the images. The background spectra were obtained from the same regions in plates free from other bright sources. Thereafter, the background spectral correction was implemented utilizing the *specgroup* task.

Finally for all of the studied stars, we have three spectra extracted from EPIC-PN, EPIC-MOS1 and EPIC-MOS2 images. The EPIC-PN, EPIC-MOS1 and EPIC-MOS2 spectra obtained on different dates were merged using the *epicspeccombine* task in case a star was observed several times.

3 SPECTRAL MODELING

The stellar X-ray spectra are approximated using the "XSPEC 12.10.0" package. All EPIC-PN, EPIC-MOS1 and EPIC-MOS2 spectra were fitted simultaneously in the 0.2–8 keV range. We applied thermal plasma models Astrophysical Plasma Emission Code (APEC, Smith et al. 2001) or MEKAL (Mewe et al. 1985; Mewe et al. 1986; Liedahl et al. 1995) for fitting. The first model describes an emission spectrum from collisionally-ionized diffuse gas. MEKAL is a model of an emission spectrum from hot diffuse gas based on the calculations of Mewe and Kaastra with Fe L calculations by Liedahl et al. (1995).

Both models have the following parameters:

T – plasma temperature in keV;

$norm$ – normalized parameter, which depends on emission measure and determines the fraction of plasma with temperature *T*;

$Abundance$ – metal abundance parameter in plasma, the plasma element abundances are obtained by multiplying the data taken from Anders & Grevesse (1989) by parameter $Abundances$.

The stellar spectra were approximated by the sum from one to three thermal models with common $Abundance$. The mean hot plasma temperatures were calculated by the following expressions:

$$T_{\rm norm} = \frac{T_1 \cdot norm_1 + T_2 \cdot norm_2}{norm_1 + norm_2}, \qquad (1)$$

or

$$T_{\rm norm} = \frac{T_1 \cdot norm_1 + T_2 \cdot norm_2 + T_3 \cdot norm_3}{norm_1 + norm_2 + norm_3}, \qquad (2)$$

where indexes 1, 2 and 3 refer to different plasma components.

For taking into account the interstellar absorption, we add to the sums of thermal models the WABS model by Morrison & McCammon (1983) or the TBABS models by Wilms et al. (2000). The first one is a model of photoelectric absorption without including Thomson scattering. The TBABS model presents the cross section for X-ray absorption by the interstellar medium (ISM) as the sum of cross sections for X-ray absorption due to gas-phase ISM, grain-phase ISM and molecules in the ISM. The parameter implemented in both models is hydrogen column density $N_{\rm H}$ in units of 10^{22} cm^{-2}. In addition, local X-ray absorption in the circumstellar surroundings was estimated. To do this, we subtracted interstellar $N_{\rm H}$ values from the $N_{\rm H}$ values obtained in the WABS or TBABS models, calculated via the following expression

$$N_{\rm H} = E(B-V) 6.12{\times}10^{21}\ {\rm cm}^2. \qquad (3)$$

This relation and color excess $E(B-V)$ are adopted from the catalog by Gudennavar et al. (2012).

In case the hydrogen column density determined by us appeared to be less then the corresponding value from the catalog by Gudennavar et al. (2012), we applied the fixed $N_{\rm H}$ parameter taken from this catalog in the WABS/TBABS models. Then we multiplied the sum of the thermal models together with this fixed parameter by the additional photoelectric absorption model PHABS for determining the local $N_{\rm H}$. For some objects, we were unable to calculate this value because $E(B-V) = 0$ or these stars are not included in the catalog by Gudennavar et al. (2012).

The results of spectral modeling are expressed in Table 2. The examples of spectral fitting are plotted in

[1] `http://simbad.u-strasbg.fr/Simbad`
[2] `http://vizier.u-strasbg.fr/viz-bin/VizieR?-source=I/345`
[3] `www.cosmos.esa.int/web/xmm-newton`

Table 1 The List of Studied Objects and Their Parameters

Star	Sp. Type	v_∞ (km s^{-1})	Ref	$\log(\dot{M})$ ($M_\odot$ yr^{-1})	Ref	B_p (G)	Ref	d (kpc)	Ref	Note
(1)	(2)	(3)	(4)	(5)	(6)	(7)	(8)	(9)	(10)	(11)
BD-60501	O7v((f))									
CPD-282561	O6.5f?p	2400	Wade et al. (2015)	–6.0	Wade et al. (2015)			5.03	G	
Tr16-22	O8.5V	2742		–7.0	Nazé et al. (2014)	1500	Nazé et al. (2014)	2.3	G	
HD 108	O6f?p	1960	Howarth et al. (1997)	–7.0	Martins et al. (2010)	1200	Martins et al. (2010)	3.8	G	
HD 14947	O5If+	2350	Repolust et al. (2004)	–5.1	Repolust et al. (2004)			3.8	G	Double
HD 15558	O4.5III(f)	2735	Howarth et al. (1997)					2.2	G	Double, PACWB
HD 15570	O4If+	2200	Bouret et al. (2012)	–5.7	Bouret et al. (2012)			2.2	G	
HD 15629	O5 V ((f))	3200	Repolust et al. (2004)	–5.9	Repolust et al. (2004)			2.2	G	
HD 16691	O4If	2300	Markova et al. (2005)	–4.9	Markova et al. (2005)			2.3	G	
HD 24912	O7.5 III(n)((f))	2450	Repolust et al. (2004)	–6.0	Repolust et al. (2004)			0.1	H	
HD 34078	O9.5V	800	Martins et al. (2005)	–9.5	Martins et al. (2005)			0.4	G	VS
HD 36512	O9.7V	2220	Fierro-Santillán et al. (2018)	–8.1	Fierro-Santillán et al. (2018)			0.5	H	
HD 36861	O8 III ((f))	2175	Howarth et al. (1997)							
HD 37043	O9III	2300	Markova et al. (2004)	–5.9	Markova et al. (2004)			0.4	H	
HD 37468	O9.5V	1500	Najarro et al. (2011)	–9.7	Najarro et al. (2011)			0.35	H	Double
HD 37742	O9.7 Ib	2100	Pollock (2007)	–5.9	Pollock (2007)					Triple
HD 45314	O9:pe	2410	Vink et al. (2009)	–7.4	Vink et al. (2009)			2.1	G	γ Cas analog
HD 47129	O8I+O7.5III	3567	Nazé et al. (2014)	–7.2	Nazé et al. (2014)	2.8	Petit et al. (2013)	0.7	G	Double
HD 47839	O7V((f))	2150	Lamers et al. (1999)	–6.2	Lamers et al. (1999)			0.3	H	
HD 54662	O6.5 V	2456	Howarth et al. (1997)					1.3	H	Double
HD 54879	O9.7V	1700	Shenar et al. (2017)	–9.0	Shenar et al. (2017)	2000	Shenar et al. (2017)	1.16	H	
HD 57682	O9 IV	1200	Grunhut et al. (2009)	–8.9	Grunhut et al. (2009)	880	Grunhut et al. (2009)	1.6	H	
HD 66811	O4 I (n)f	2485	Howarth et al. (1997)	–5.1	Repolust et al. (2004)			0.42	H	VS
HD 93128	O3.5V((fc))z	3100	Repolust et al. (2004)	–5.6	Repolust et al. (2004)			3.5	H	
HD 93129	O2If*+O3.5V((f))	3200	Repolust et al. (2004)	–4.5	Repolust et al. (2004)			2.3	Gagné et al. (2011)	Double, PACWB
HD 93205	O3.5V((f))+O8V	3200	Garcia & Bianchi (2004)	–6.5	Garcia & Bianchi (2004)			3.3	G	
HD 93250	O4III(fc)	3250	Repolust et al. (2004)	–5.5	Repolust et al. (2004)			2.3	G	PACWB
HD 93403	O5.5I+O7V	2615	Howarth et al. (1997)	–3.3	Rauw et al. (2002)	42	Hubrig et al. (2011)			Double
HD 93521	O9.5Vp	400	Howarth et al. (1997)			126	Hubrig et al. (2013)	1.8	G	
HD 101205	O7IIIn((f))	2740	Howarth et al. (1997)					2.4	H	Double, β Lyr
HD 148937	O6.5f?p	2600	Nazé et al. (2008)	–5.5	Nazé et al. (2014)	1000	Petit et al. (2013)	1.4	G	
HD 152233	O6II(f)	2730	Howarth et al. (1997)			106	Hubrig et al. (2011)	2.3	G	Double
HD 152248	O7Iabf+O7Ib(f)	2420	Howarth et al. (1997)	–5.5	Sana et al. (2004)			2.2	G	Double, β Lyr
HD 152249	O9Ib((f))	2010	Howarth et al. (1997)			27	Hubrig et al. (2011)	1.9	G	
HD 152408	O8: Ia fpe	955	Howarth et al. (1997)	–4.7	Prinja et al. (2001)			1.9	H	PACWB
HD 155806	O7.5 V [n]e	2460	Howarth et al. (1997)			115	Hubrig et al. (2011)	0.86	G	
HD 159176	O7 V((f))	2590	Howarth et al. (1997)	–5.5				1.06	H	Double
HD 164794	O7.5III+ O9.5III+O9.5	2750	Howarth et al. (1997)					1.6	G	Triple, PACWB
HD 166734	O7.5If+O9I(f)	1331	Nazé et al. (2017)	–5.0	Nazé et al. (2017)			0.72	G	Double
HD 167971	O8Iaf(n)+O4	2185	Howarth et al. (1997)	–5.9				0.77	G	Double, PACWB
HD 188001	O7.5 Ia f	1980	Howarth et al. (1997)					2.8	G	
HD 191612	O6f?p-O8fp	2700	Sundqvist et al. (2012)	–5.8	Sundqvist et al. (2012)			2.3	G	
HD 210839	O6 I (n)fp	2300	Howarth et al. (1997)	–5.2	Repolust et al. (2004)			1.1	G	
HD 215835	O6 V (n)	2810	Howarth et al. (1997)					3.5	G	Double
CD-2312861	B2IV+B2V	700	Pillitteri et al. (2018)	–9.9	Pillitteri et al. (2018)	500	Pillitteri et al. (2018)	0.11	H	Double
BD-124982	B0II	1350	Bertout et al. (1985)	–5.8	Bertout et al. (1985)			1.8	G	
HD 3360	B2IV	942	Nazé et al. (2014)	–8.4	Nazé et al. (2014)	340	Petit et al. (2013)	0.18	H	PVS
HD 5394	B0.5IVe							0.19	H (1997)	γ Cas
HD 10144	B3 Ve	1330	Cohen et al. (1997)	–10.4	Cohen et al. (1997)			0.04	H	Be
HD 21856	B1V	500	De Becker et al. (2017)	–8.2	De Becker et al. (2017)			0.5	G	
HD 24398	Bl Ib	1295	Howarth et al. (1997)					0.23	H	VS
HD 24760	B1.5III							0.2	H	
HD 33328	B2III(e)p							0.25	H	
HD 34816	B0.5V							0.26	H	
HD 35468	B2V							0.08	H	
HD 36959	B1.2							0.5	G	
HD 36960	B1/2Ib/II							0.57	H	
HD 37000	B3/5							0.41	G	
HD 37025	B3(III)							0.35	G	
HD 37061	B0.5V	2901	Nazé et al. (2014)	–8.1	Nazé et al. (2014)	650	Petit et al. (2013)	0.4	G	
HD 37128	B0 la	1910	Howarth et al. (1997)	–5.6	Petit et al. (2013)			0.41	H	BS
HD 37479	B2Vp	1794	Nazé et al. (2014)	–9.8	Nazé et al. (2014)	9600	Petit et al. (2013)	0.46	G	
HD 46328	B1 III	1984	Kurapati et al. (2017)			1500	Petit et al. (2013)	0.46	H	β Cep
HD 44743	B1II-III			–8.2	Drew et al. (1994)	100	Fossati et al. (2015)	0.15	H	
HD 50707	B1Ib						0.5	H		
HD 52089	B1 II/III			–8.1	Drew et al. (1994)	13	Fossati et al. (2015)	0.12	H	
HD 63425	B0.5V	2478	Nazé et al. (2014)	–7.9	Nazé et al. (2014)	460	Petit et al. (2013)	1.11	G	
HD 63922	BIII						0.51	H		
HD 64760	B0.5 Ib	1500	Howarth et al. (1997)					1.06	H	
HD 66665	B0.5V	2008	Nazé et al. (2014)	–8.2	Nazé et al. (2014)	670	Petit et al. (2013)	1.5	G	
HD 79351	B2IV-V						0.14	H		
HD 105382	B3/5III					2300	Alecian et al. (2011)	0.10	G	
HD 111123	B1IV	2000	Cohen et al. (2008)	–8	Cohen et al. (2008)			0.09	H	
HD 116658	B1IV	1750	Cohen et al. (1997)	–8.0	Cohen et al. (1997)			0.08	H	β Cep
HD 120324	B2IV-Ve	1470	Cohen et al. (1997)	–9.1	Cohen et al. (1997)			0.16	H	Be
HD 120991	B2Ve							7.95	G	

Table 1 *Continued.*

Star	Sp. Type	v_∞ (km s^{-1})	Ref	$\log(\dot{M})$ ($M_\odot$ yr^{-1})	Ref	B_p (G)	Ref	d (kpc)	Ref	Note
(1)	(2)	(3)	(4)	(5)	(6)	(7)	(8)	(9)	(10)	(11)
HD 122451	B1III	1552	Nazé et al. (2014)	–8.0	Nazé et al. (2014)	250	Petit et al. (2013)	0.12	H	β Cep
HD 127381	B1-2V	2186	Nazé et al. (2014)	–9.7	Nazé et al. (2014)	500	Petit et al. (2013)	0.18	H	EVS
HD 136504	B2IV-V	1019	Nazé et al. (2014)	–8.3	Nazé et al. (2014)	600	Petit et al. (2013)	0.16	H	Double
HD 143275	B0.2IVe	1100	De Becker et al. (2017)	–6.9	De Becker et al. (2017)		-	0.15	H	
HD 144217	B0.5V	1430	Bertout et al. (1985)	–6.8	Bertout et al. (1985)			0.12	H	
HD 147932	B5					3000	Alecian et al. (2014)	0.13	G	
HD 149438	B0.2V	2176	Nazé et al. (2014)	–7.6	Nazé et al. (2014)	200	Petit et al. (2013)	0.15	H	
HD 152234	B0.5Ia	1450	Howarth et al. (1997)					1.9	H	
HD 157246	B1 Ib	735	Howarth et al. (1997)					0.35	H	
HD 158926	B1.5 IV	1560	Cohen et al. (1997)	–8.4	Cohen et al. (1997)			0.18	H	β Cep
HD 165024	B2 Ib	1185	Howarth et al. (1997)					0.25	H	
HD 175191	B3 IV	1220	Cohen et al. (1997)	–9.9	Cohen et al. (1997)			0.07	H	HPM
HD 182180	B2Vn	1058	Nazé et al. (2014)	–9.9	Nazé et al. (2014)	11000	Petit et al. (2013)	0.23	G	
HD 193924	B2.5V	1360	Cohen et al. (1997)	–9.9	Cohen et al. (1997)			0.05	H	Double
HD 200775	B2Ve	862	Nazé et al. (2014)	–8.1	Nazé et al. (2014)	1000	Petit et al. (2013)	0.4	G	HAEBE
HD 205021	B1IV	2169	Nazé et al. (2014)	–8.6	Nazé et al. (2014)	360	Petit et al. (2013)	0.21	H	β Cep
HD 261938	B3V							0.72	G	

The names of stars can be found in Col. (1). The spectral types are given in Col. (2). Cols. (3), (5) and (7) consist of terminal wind velocity, mass loss rate and polar magnetic field respectively. Sources of these values are reported in Cols. (4), (6) and (8) respectively. Cols. (9) and (10) express distances to the stars and sources of the values respectively. References: PVS – Pulse variable stars; VS – Variable stars; BS – Blue supergiants; EVS – Ellipsoidal variable stars; HAEBE – Ae/Be Herbig stars; β Lyr – Double stars of β Lyr type; HPM – High proper motion stars; G – distances from Gaia DR2 online catalog (2018); H, H (1997) – distances from the Hipparcos catalog by van Leeuwen (2007) and by Perryman et al. (1997) respectively.

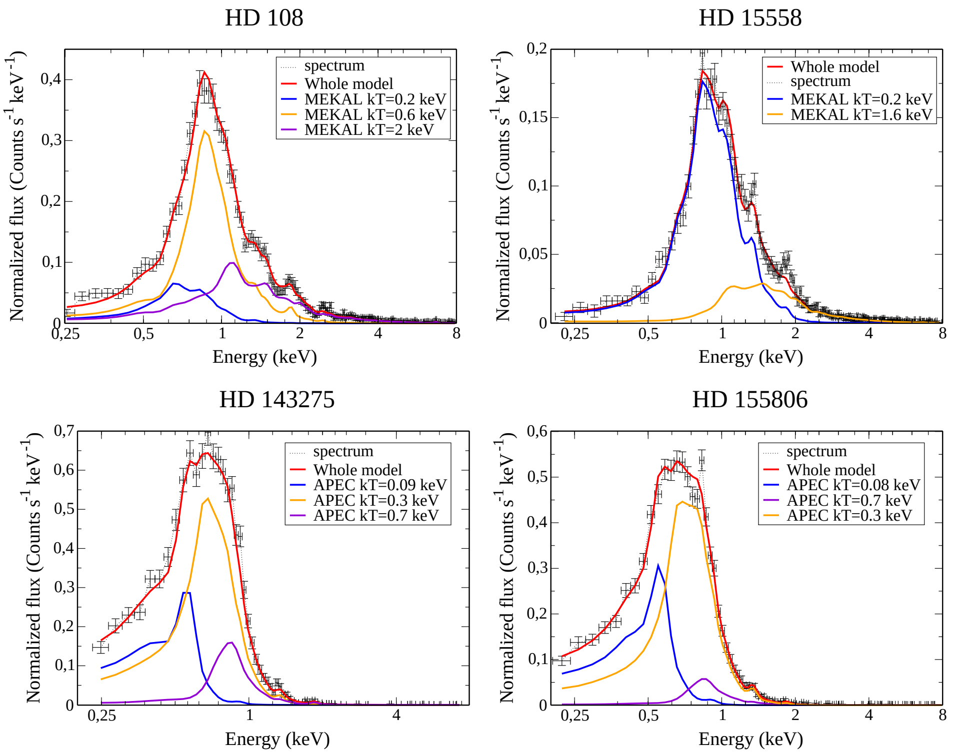

Fig. 1 Examples of spectral fitting by the thermal models. The contributions of individual components (*blue*, *dark yellow* and *magenta lines*) to the total model X-ray spectra (*red line*) are presented.

Figure 1. The contributions of different components to the total X-ray spectra are depicted.

Also, we calculated stellar X-ray luminosity in the 0.2–8 keV range using the standard expression

$$L_{\rm X} = 4\pi D^2 F \,{\rm erg\,s^{-1}}, \qquad (4)$$

where D is distance to the star in cm (distances in kpc are given in Table 1) and F is the integral observed flux in the mentioned range. Inasmuch as a main part of X-ray emission from OB-type stars is concentrated in the energy range of about 0.2–2 keV, the X-ray luminosity in 0.2–8 keV energies almost exactly corresponds to the total X-ray luminosity of the star. Our estimations demonstrate that a contribution of X-rays out of the 0.2–8 keV interval does not exceed 1% of the total X-ray flux.

Table 2 Log of observations. The object names are given in Cols. (1) and (5). ID numbers of observations are presented in Cols. (2) and (6). Dates and exposure times are provided in Cols. (3)–(4) and (7)–(8) respectively.

Star (1)	ObsID (2)	Date (3)	Exp (s) (4)	Star (5)	ObsID (6)	Date (7)	Exp (s) (8)
HD 108	109120101	21.08.2002	36685	HD 122451	150020101	19.07.2003	57623
HD 3360	600530301	03.08.2009	13000	HD 127381	690210101	10.08.2012	8000
HD 5394	201220101	05.02.2004	71037	HD 136504	690210201	04.03.2013	9000
	651670301	24.07.2010	16115	HD 143275	743660101	07.03.2015	31200
	651670401	02.08.2010	17914	HD 144217	690200301	06.03.2013	31921
	651670501	20.08.2010	23818	HD 148937	22140101	25.02.2001	16507
	743600101	24.07.2014	34000		22140501	25.02.2001	10531
HD 10144	42120101	07.12.2006	13680		22140601	25.02.2001	14610
HD 14947	690880101	20.01.2013	21917	HD 149438	112540101	20.08.2001	19001
HD 15558	740020101	25.08.2014	50000		112540201	20.08.2001	7300
HD 16691	671100101	21.08.2011	21719	HD 152233	109490101	05.09.2001	33870
HD 21856	743660301	03.03.2015	33000	HD 152234	109490201	06.09.2001	33773
HD 24398	201550201	13.02.2004	41100	HD 152248	109490301	07.09.2001	35009
HD 24760	761090801	16.08.2015	17000	HD 152249	109490401	08.09.2001	31873
HD 33328	402120301	18.03.2007	14917		109490501	09.09.2001	31664
HD 33904	143370101	23.03.2003	47265		109490601	10.09.2001	33505
HD 34078	206360101	10.09.2004	58938	HD 152408	602020101	30.08.2009	36914
HD 34816	690200601	15.02.2013	31921		603570401	31.07.2009	33917
HD 35468	690680501	22.09.2012	50806	HD 155806	554440101	26.08.2008	36913
HD 36512	690200201	22.08.2012	29964		561380601	08.10.2013	68800
HD 36861	402050101	28.09.2006	56214		159360101	30.05.2003	72876
HD 36960	690200501	23.03.2013	44433		1730301	09.03.2001	9362
HD 37043	112660101	15.09.2001	23217		1730401	09.03.2001	10859
	112660201	14.09.2001	7576	HD 157246	201550101	22.02.2004	27600
HD 37061	93000101	25.03.2001	74939				
	93000301	26.03.2001	17912	HD 158926	690200101	04.03.2013	31200
HD 37128	112400101	06.03.2002	13153				
HD 37468	101440301	23.03.2002	43820		691760101	08.09.2012	22917
HD 37479	101440301	23.03.2002	43820	HD 164794	720540401	08.03.2013	21916
HD 37742	657200101	03.09.2010	97810		720540501	03.09.2013	26700
	657200201	03.09.2011	47415		720540601	05.03.2014	27500
	657200301	29.08.2012	43912	HD 165024	302020201	12.10.2005	72700
HD 44743	503500101	06.03.2008	20063	HD 166734	500030101	05.03.2008	73368
	761090101	21.04.2015	113000		500030201	05.03.2008	6947
					790180601	02.04.2016	12000
HD 46328	691900101	16.10.2012	102000	HD 167971	740990101	09.09.2014	26800
HD 47129	1730501	17.09.2002	21939				
	1730601	16.03.2003	21863	HD 182180	690210401	25.09.2012	12000
HD 47777	11420101	20.03.2001	41413	HD 188001	743660201	14.10.2014	33000
	11420201	17.03.2002	41760		740180701	30.05.2014	17900
HD 47839	11420101	20.03.2001	41413	HD 191612	300600201	05.04.2005	28376
HD 50707	761091201	15.09.2015	17400		300600301	02.06.2005	23813
HD 52089	69750101	19.03.2001	47013		300600401	08.10.2005	28915
HD 54662	743660501	01.10.2014	33900		300600501	17.04.2005	21775
HD 54879	780180101	01.05.2016	40100	HD 193924	690680201	20.03.2013	71000
HD 57682	650320201	16.10.2010	11914	HD 200775	650320101	30.08.2010	11916
				HD 205021	300490201	27.07.2005	41100
HD 63425	671990201	06.05.2011	21200		300490301	29.07.2005	39300
HD 63922	720390601	15.11.2013	55000		300490401	02.08.2005	43200
HD 64760	401050201	16.03.2007	68788		300490501	06.08.2005	41100
HD 66665	671990101	29.10.2011	37700	HD 210839	720090301	03.08.2013	77000
HD 66811	561380201	07.10.2010	76914		720090401		
HD 79351	690200701	02.01.2013	54915		720090501	05.08.2013	96900
HD 93030	101440201	13.08.2002	44325	HD 212571	720390701	17.11.2013	54500
HD 93129	804950201	04.06.2017	33000	HD 215835	205650101	19.12.2003	31413
	804950301	06.12.2017	3000	BD-124982	8820301	07.04.2002	13733
HD 93403	109530101	24.12.2000	10002		8820601	09.09.2002	13951
	109530201	28.12.2000	9817	CD-2312861	760900101	22.02.2016	141900
	109530301	31.12.2000	9909		720690101	29.08.2013	53000
	109530501	31.12.2000	9211	CPD-282561	740180501	04.05.2014	24000
HD 93521	600620101	02.11.2009	41812		740180601	14.05.2014	12999
HD 101205	672060101	01.01.2012	41910				
				Tr16-22	112560101	25.06.2001	37052
HD 116658	690680101	06.07.2012	13000		112560301	30.06.2001	37714
					160160901	13.06.2003	31655
HD 120324	402121701	15.02.2007	11150		311990101	31.01.2006	66949
HD 120991	402121801	25.01.2007	10951		560580301	15.01.2009	26917

Table 3 Parameters of Model Fit for Program Stars

Star	$N_{\rm H}^{\rm local}$ (10^{22} cm^{-2})	kT_1 (keV)	$norm_1$ (10^{-4})	kT_2 (keV)	$norm_2$ (10^{-4})	kT_3 (keV)	$norm_3$ (10^{-4})	Abundance (solar units)	χ^2 (d.o.f.)
O-type stars									
HD 108	$0.061^{+0.058}_{-0.058}$	$0.63^{+0.12}_{-0.03}$	$7.18^{+3.00}_{-3.41}$	$2.09^{+0.14}_{-0.12}$	$5.29^{+0.38}_{-0.48}$	$0.24^{+0.20}_{-0.06}$	$4.63^{+5.32}_{-2.85}$	$0.34^{+0.09}_{-0.08}$	1.26 (404)
HD 14947	$0.24^{+0.21}_{-0.21}$	$0.58^{+0.16}_{-0.10}$	$5.97^{+3.34}_{-1.80}$					$0.12^{+0.23}_{-0.08}$	1.05 (213)
HD 15558	$0.32^{+0.06}_{-0.06}$	$0.24^{+0.02}_{-0.02}$	199^{+87}_{-63}	$1.58^{+0.16}_{-0.12}$	$4.91^{+0.58}_{-0.61}$			$0.12^{+0.06}_{-0.04}$	1.23 (403)
HD 15570	$0.31^{+0.11}_{-0.11}$	$0.19^{+0.04}_{-0.04}$	132^{+181}_{-87}	$0.66^{+0.09}_{-0.06}$	14^{+5}_{-4}			$0.11^{+0.06}_{-0.04}$	1.23 (295)
HD 15629	$0.17^{+0.09}_{-0.09}$	$0.56^{+0.46}_{-0.18}$	$1.07^{+4.39}_{-0.96}$	$0.22^{+0.03}_{-0.03}$	43^{+49}_{-26}			$0.12^{+0.19}_{-0.05}$	0.82 (219)
HD 16691	$0.18^{+0.17}_{-0.17}$	$0.71^{+0.11}_{-0.13}$	$5.09^{+3.09}_{-1.48}$					$0.06^{+0.12}_{-0.04}$	0.77 (199)
HD 34078	$0.095^{+0.028}_{-0.028}$	$0.76^{+0.14}_{-0.13}$	$0.05^{+0.04}_{-0.03}$	$0.27^{+0.01}_{-0.01}$	$2.55^{+1.58}_{-0.35}$	$0.14^{+0.01}_{-0.01}$	$4.83^{+2.97}_{-1.16}$	≤ 3.16	1.72 (334)
HD 36512	≤ 0.014	$0.14^{+0.01}_{-0.01}$	36^{+16}_{-6}	$0.29^{+0.01}_{-0.01}$	23^{+5}_{-5}			$0.17^{+0.05}_{-0.03}$	1.17 (262)
HD 47129	≤ 0.003	$2.77^{+0.31}_{-0.21}$	14^{+2}_{-2}	$0.31^{+0.03}_{-0.03}$	22^{+3}_{-7}	$0.92^{+0.02}_{-0.01}$	26^{+3}_{-4}	$0.19^{+0.03}_{-0.03}$	1.64 (436)
HD 47839	$0.03^{+0.02}_{-0.02}$	$0.245^{+0.007}_{-0.007}$	58^{+13}_{-12}	≤ 0.096	381^{+100}_{-230}	$0.68^{+0.05}_{-0.09}$	$2.75^{+1.69}_{-0.67}$	$0.19^{+0.05}_{-0.04}$	1.57 (238)
HD 54662	≤ 0.06	$0.187^{+0.009}_{-0.008}$	10^{+7}_{-5}	$0.59^{+0.03}_{-0.03}$	$1.92^{+0.89}_{-0.92}$			$0.78^{+0.80}_{-0.29}$	1.42 (280)
HD 54879	$0.14^{+0.08}_{-0.08}$	$0.18^{+0.02}_{-0.02}$	$5.70^{+3.14}_{-2.10}$	$0.74^{+0.03}_{-0.03}$	$2.63^{+0.72}_{-0.82}$			$0.46^{+0.40}_{-0.17}$	1.14 (330)
HD 57682	$0.05^{+0.02}_{-0.04}$	$0.69^{+0.09}_{-0.03}$	13^{+2}_{-4}					$0.096^{+0.020}_{-0.017}$	1.00 (280)
HD 93128‡	$0.57^{+0.08}_{-0.09}$	$1.96^{+0.42}_{-0.35}$	532^{+375}_{-190}	$0.24^{+0.05}_{-0.03}$	165^{+170}_{-84}			$0.05^{+0.04}_{-0.02}$	1.01 (260)
HD 93129	$0.60^{+0.04}_{0.04}$	$0.149^{+0.008}_{-0.005}$	1046^{+407}_{-310}	$0.52^{+0.02}_{-0.02}$	84^{+12}_{-11}	$2.45^{+0.16}_{-0.14}$	$16.5^{+1.2}_{-1.2}$	$0.17^{+0.03}_{-0.02}$	1.69 (465)
HD 93205	$0.27^{+0.05}_{-0.05}$	$0.16^{+0.01}_{-0.01}$	126^{+53}_{-40}	$0.61^{+0.02}_{-0.02}$	$12.8^{+1.6}_{-1.5}$			$0.28^{+0.07}_{-0.06}$	1.75 (413)
HD 93250	$0.17^{+0.08}_{-0.08}$	$0.16^{+0.03}_{-0.02}$	179^{+200}_{-113}	$0.59^{+0.03}_{-0.02}$	52^{+9}_{-10}	$4.02^{+1.16}_{-0.82}$	$7.15^{+1.48}_{-1.13}$	$0.12^{+0.05}_{-0.03}$	1.24 (297)
HD 93403‡	$0.53^{+0.14}_{-0.05}$	$0.30^{+0.03}_{-0.02}$	71^{+34}_{-24}	$1.96^{+0.32}_{-0.28}$	$9.46^{+3.14}_{-2.17}$	$0.78^{+0.04}_{-0.03}$	$24.72^{+5.64}_{-6.04}$	$0.26^{+0.08}_{-0.05}$	1.55 (305)
HD 93521	$0.15^{+0.06}_{-0.06}$	$0.25^{+0.06}_{-0.03}$	14^{+12}_{-9}					$0.014^{+0.010}_{-0.007}$	0.99 (279)
HD 101205	$0.22^{+0.06}_{-0.06}$	$0.17^{+0.01}_{-0.01}$	54^{+31}_{-20}	$0.61^{+0.03}_{-0.10}$	$9.42^{+1.62}_{-1.43}$	$1.13^{+0.06}_{-0.18}$	$4.13^{+3.25}_{-0.69}$	$0.36^{+0.10}_{-0.08}$	1.14 (399)
HD 148937	$0.07^{+0.05}_{-0.05}$	$0.19^{+0.02}_{-0.01}$	66^{+42}_{-32}	$0.60^{+0.01}_{-0.01}$	47^{+8}_{-7}	$2.09^{+0.08}_{-0.07}$	30^{+1}_{-2}	$0.39^{+0.05}_{-0.05}$	1.68 (478)
HD 152233	$0.39^{+0.03}_{-0.03}$	$0.121^{+0.007}_{-0.005}$	235^{+92}_{-66}	$0.51^{+0.02}_{-0.02}$	$6.34^{+1.73}_{-1.65}$			$0.86^{+0.36}_{-0.21}$	1.81 (354)
HD 152248	$0.24^{+0.06}_{-0.06}$	$0.15^{+0.01}_{-0.01}$	89^{+41}_{-27}	$0.60^{+0.03}_{-0.03}$	11^{+4}_{-4}			$0.73^{+0.61}_{-0.27}$	1.02 (263)
HD 152249	$0.13^{+0.08}_{-0.08}$	$0.23^{+0.04}_{-0.04}$	28^{+20}_{-20}	$0.57^{+0.10}_{-0.10}$	$4.7^{+2.5}_{-2.5}$			$0.26^{+0.14}_{-0.14}$	1.10 (226)
HD 152408	$0.97^{+0.33}_{-0.33}$	$1.71^{+0.32}_{-0.32}$	$0.31^{+0.24}_{-0.11}$	$0.56^{+0.01}_{-0.09}$	$2.64^{+0.54}_{-0.54}$			$0.85^{+0.21}_{-0.60}$	1.16 (259)
HD 155806	$0.15^{+0.04}_{-0.04}$	$0.078^{+0.013}_{-0.009}$	47^{+133}_{-28}	$0.25^{+0.02}_{-0.01}$	$1.88^{+4.21}_{-0.54}$	$0.69^{+0.15}_{-0.07}$	$0.07^{+0.28}_{-0.04}$	≤ 0.99	0.93 (332)
HD 159176	$0.07^{+0.03}_{-0.03}$	$0.20^{+0.02}_{-0.01}$	51^{+20}_{-14}	$0.94^{+0.10}_{-0.05}$	14^{+3}_{-5}	$0.54^{+0.08}_{-0.08}$	15^{+5}_{3}	$0.26^{+0.05}_{-0.04}$	1.3 (336)
HD 164794	$0.04^{+0.02}_{-0.02}$	$0.79^{+0.05}_{-0.04}$	25^{+3}_{-3}	$0.264^{+0.008}_{-0.007}$	183^{+42}_{-33}			$0.11^{+0.01}_{-0.01}$	1.88 (409)
HD 167971	$0.32^{+0.04}_{-0.04}$	$1.01^{+0.03}_{-0.03}$	41^{+4}_{-4}	$0.23^{+0.01}_{-0.01}$	431^{+122}_{-100}			$0.40^{+0.07}_{-0.06}$	1.58 (411)
HD 188001	$0.44^{+0.04}_{-0.04}$	$0.24^{+0.01}_{-0.01}$	14^{+3}_{-2}					1 (fr.)	1.7 (272)
HD 191612	≤ 0.03	$0.47^{+0.06}_{-0.06}$	$6.59^{+2.26}_{-1.70}$	$0.83^{+0.11}_{-0.07}$	$4.36^{+1.64}_{-2.05}$	$2.30^{+0.18}_{-0.13}$	$5.47^{+0.46}_{-0.48}$	$0.26^{+0.04}_{-0.04}$	1.31 (458)
HD 210839	$0.43^{+0.02}_{-0.02}$	$0.118^{+0.005}_{-0.003}$	854^{+284}_{-215}	$0.48^{+0.01}_{-0.01}$	17^{+4}_{-4}			$0.93^{+0.31}_{-0.20}$	1.59 (380)
HD 215835	$0.33^{+0.08}_{-0.08}$	$0.24^{+0.02}_{-0.02}$	30^{+23}_{-15}	$0.79^{+0.09}_{-0.06}$	$2.89^{+1.67}_{-1.44}$			$0.85^{+1.44}_{-0.41}$	1.16 (276)
BD-60501	≤ 0.05	$0.71^{+0.05}_{-0.12}$	$1.43^{+0.88}_{-0.31}$					$0.13^{+0.06}_{-0.04}$	1.08 (222)
CPD-282561‡	$0.39^{+0.08}_{-0.08}$	$2.34^{+0.70}_{-0.39}$	$1.15^{+0.25}_{-0.30}$	$0.90^{+0.10}_{-0.13}$	$0.58^{+0.70}_{-0.27}$			$0.29^{+0.21}_{-0.14}$	1.11 (330)
Tr16-22	$0.22^{+0.19}_{-0.19}$	$1.82^{+0.17}_{-0.22}$	$2.84^{+0.85}_{-0.59}$	$0.81^{+0.25}_{-0.08}$	$1.69^{+1.01}_{-0.80}$			$0.53^{+0.33}_{-0.33}$	0.95 (387)
B-type stars									
HD 3360	$0.047^{+0.046}_{-0.046}$	$0.32^{+0.05}_{-0.05}$	$5.30^{+6.46}_{-1.93}$					$0.031^{+0.021}_{-0.017}$	1.04 (242)
HD 10144	≤ 0.08	$0.33^{+0.05}_{-0.03}$	30^{+15}_{-12}					$0.07^{+0.02}_{-0.02}$	1.39 (216)
HD 21856	$0.12^{+0.09}_{-0.09}$	$0.38^{+0.27}_{-0.09}$	$1.89^{+4.20}_{-1.50}$					$0.023^{+0.31}_{-0.19}$	0.95 (134)
HD 24760	$0.065^{+0.024}_{-0.024}$	$0.24^{+0.01}_{-0.01}$	142^{+59}_{-35}					$0.023^{+0.007}_{-0.006}$	1.67 (206)
HD 33328	$0.070^{+0.068}_{-0.068}$	$0.95^{+0.16}_{-0.12}$	$0.66^{+0.43}_{-0.24}$	$0.22^{+0.06}_{-0.04}$	$1.10^{+3.49}_{-0.52}$			$0.14^{+0.13}_{-0.09}$	0.92 (204)
HD 33904‡	$0.015^{+0.005}_{-0.004}$	$1.022^{+0.015}_{-0.015}$	$10.71^{+0.52}_{-0.50}$	$0.27^{+0.01}_{-0.01}$	$8.50^{+0.83}_{-0.74}$			$0.15^{+0.01}_{-0.01}$	1.44 (402)
HD 34816	≤ 0.006	$0.26^{+0.02}_{-0.01}$	$7.26^{+3.74}_{-3.10}$	$0.11^{+0.01}_{-0.02}$	21^{+20}_{-7}			$0.23^{+0.19}_{-0.08}$	1.05 (241)

Table 3 *Continued.*

Star	$N_{\rm H}^{\rm local}$ (10^{22} cm^{-2})	kT_1 (keV)	$norm_1$ (10^{-4})	kT_2 (keV)	$norm_2$ (10^{-4})	kT_3 (keV)	$norm_3$ (10^{-4})	Abundance (solar units)	χ^2 (d.o.f.)
HD 35468‡	$0.066^{+0.26}_{-0.017}$	≤ 0.096	57^{+42}_{-21}	$0.29^{+0.02}_{-0.02}$	$3.21^{+1.54}_{-1.34}$			$0.16^{+0.14}_{-0.07}$	1.35 (276)
HD 36959	$0.038^{+0.014}_{-0.014}$	$0.81^{+0.04}_{-0.05}$	$3.69^{+0.57}_{-0.44}$					$0.055^{+0.015}_{-0.014}$	1.12 (276)
HD 36960	≤ 0.013	$0.31^{+0.02}_{-0.02}$	$6.90^{+1.26}_{-0.98}$	$0.093^{+0.10}_{-0.007}$	27^{+17}_{-7}	$1.32^{+0.04}_{-0.04}$	$6.99^{+0.48}_{-0.43}$	$0.18^{+0.03}_{-0.03}$	1.3 (377)
HD 37000‡	$0.29^{+0.04}_{-0.04}$	$0.68^{+0.05}_{-0.04}$	823^{+258}_{-197}					$0.20^{+0.07}_{-0.05}$	1.15 (233)
HD 37025‡	$0.045^{+0.044}_{-0.033}$	$0.77^{+0.07}_{-0.08}$	$0.57^{+0.31}_{-0.21}$					$0.17^{+0.13}_{-0.07}$	0.98 (165)
HD 37061†	0.33 (fr.)	$1.29^{+0.34}_{-0.34}$	$0.75^{+0.54}_{-0.54}$	$0.29^{+0.06}_{-0.06}$	$2.11^{+1.69}_{-1.69}$			$1.21^{+1.11}_{-1.11}$	0.77 (147)
HD 37479	$0.020^{+0.008}_{-0.008}$	$5.45^{+1.37}_{-0.92}$	$6.17^{+1.05}_{-0.84}$	$0.27^{+0.03}_{-0.01}$	$5.67^{+1.51}_{-1.31}$	$1.23^{+0.04}_{-0.05}$	$7.97^{+1.81}_{-1.97}$	$0.15^{+0.05}_{-0.03}$	1.17 (469)
HD 46328	$0.034^{+0.012}_{-0.012}$	$0.11^{+0.01}_{-0.01}$	16^{+13}_{-4}	$0.31^{+0.01}_{+0.01}$	$6.19^{+0.62}_{-0.55}$	$0.81^{+0.02}_{-0.01}$	$3.95^{+0.32}_{-0.32}$	$0.35^{+0.03}_{-0.03}$	1.43 (401)
HD 47777†	0.05 (fr.)	$1.32^{+0.20}_{-0.20}$	$0.50^{+0.11}_{-0.11}$	$0.38^{+0.10}_{-0.10}$	$0.34^{+0.14}_{-0.14}$			$0.18^{+0.11}_{-0.11}$	0.96 (265)
HD 50707	≤ 0.028	$0.21^{+0.02}_{-0.02}$	$3.95^{+3.72}_{-2.10}$					$0.078^{+0.095}_{-0.037}$	0.9 (147)
HD 63425	≤ 0.018	$0.69^{+0.12}_{-0.11}$	$0.82^{+0.65}_{-0.32}$	$0.29^{+0.05}_{-0.08}$	$1.57^{+1.51}_{-0.81}$			$0.20^{+0.09}_{-0.09}$	0.76 (224)
HD 63922	≤ 0.024	$0.27^{+0.01}_{-0.02}$	17^{+4}_{-4}	$0.13^{+0.02}_{-0.02}$	25^{+17}_{-7}	$0.71^{+0.02}_{-0.09}$	$1.44^{+0.70}_{-0.21}$	$0.21^{+0.06}_{-0.04}$	1.26 (328)
HD 64760	≤ 0.014	$0.62^{+0.02}_{-0.02}$	$4.36^{+0.47}_{-0.43}$	$0.19^{+0.01}_{-0.01}$	$4.90^{+0.95}_{-0.77}$			$0.127^{+0.016}_{-0.015}$	1.21 (359)
HD 66665	$0.045^{+0.032}_{-0.032}$	$0.61^{+0.11}_{-0.12}$	$0.010^{+0.070}_{-0.003}$	$0.18^{+0.03}_{-0.03}$	$0.03^{+0.24}_{-0.01}$			≤ 0.55	0.95 (160)
HD 79351	≤ 0.0007	$0.71^{+0.04}_{-0.06}$	$5.48^{+0.82}_{-0.80}$	$1.21^{+0.05}_{-0.06}$	$7.47^{+1.07}_{-0.91}$			$0.20^{+0.02}_{-0.02}$	1.32 (449)
HD 105382‡	≤ 0.034	$0.61^{+0.06}_{-0.10}$	$1.23^{+0.73}_{-0.23}$					$0.11^{+0.06}_{-0.05}$	0.8 (138)
HD 116658†	0.018 (fr.)	$0.090^{+0.003}_{-0.003}$	74^{+48}_{-48}	$0.25^{+0.01}_{-0.01}$	10^{+8}_{-8}			$0.76^{+0.55}_{-0.55}$	1.21 (172)
HD 120324	$0.022^{+0.009}_{-0.009}$	$1.02^{+0.10}_{-0.18}$	$1.55^{+0.76}_{-0.39}$	$0.32^{+0.05}_{-0.03}$	$2.21^{+1.92}_{-0.74}$			$0.21^{+0.13}_{-0.10}$	1.12 (214)
HD 120991	$0.059^{+0.008}_{-0.008}$	$6.25^{+0.68}_{-0.61}$	$17.37^{+0.78}_{-0.74}$	$0.85^{+0.19}_{-0.12}$	$0.99^{+0.51}_{-0.34}$			$0.45^{+0.14}_{-0.13}$	1.11 (475)
HD 127381	≤ 0.12	$0.19^{+0.02}_{-0.02}$	≤ 3.17					≤ 0.09	0.78 (66)
HD 136504‡	$0.018^{+0.012}_{-0.011}$	$1.20^{+0.09}_{-0.09}$	$9.43^{+1.16}_{-0.99}$					$0.03^{+0.02}_{-0.01}$	1.39 (248)
HD 143275‡	$0.15^{+0.05}_{-0.05}$	$0.26^{+0.01}_{-0.01}$	$1.10^{+0.98}_{-0.37}$	$0.09^{+0.02}_{-0.01}$	$6.30^{+17.45}_{-4.64}$	$0.69^{+0.06}_{-0.02}$	$0.14^{+0.11}_{-0.02}$	≤ 2.90	1.36 (211)
HD 144217‡	$0.17^{+0.03}_{-0.02}$	$0.91^{+0.03}_{-0.03}$	$9.03^{+0.77}_{-0.78}$	$0.25^{+0.01}_{-0.01}$	58^{+13}_{-11}	$0.11^{+0.01}_{-0.02}$	175^{+275}_{-173}	$0.22^{+0.03}_{-0.02}$	1.39 (424)
HD 147932	$0.12^{+0.02}_{-0.02}$	$1.03^{+0.02}_{-0.02}$	21^{+4}_{-2}	$4.97^{+1.55}_{-1.07}$	$3.98^{+0.58}_{-0.94}$			$0.11^{+0.02}_{-0.01}$	1.22 (458)
HD 152234	$0.18^{+0.06}_{-0.06}$	$0.31^{+0.09}_{-0.03}$	14^{+6}_{-7}	$0.81^{+0.03}_{-0.03}$	$3.81^{+0.57}_{-0.57}$	$0.13^{+0.04}_{-0.03}$	49^{+93}_{-26}	$0.38^{+0.07}_{-0.07}$	1.55 (384)
HD 157246	$0.06^{+0.02}_{-0.02}$	$0.18^{+0.03}_{-0.03}$	$6.26^{+5.37}_{-1.79}$	$0.62^{+0.02}_{-0.02}$	11^{+1}_{-1}			$0.14^{+0.02}_{-0.02}$	0.95 (308)
HD 158926	≤ 0.77	$0.28^{+0.02}_{-0.02}$	$2.33^{+1.76}_{-1.76}$	$0.119^{+0.008}_{-0.006}$	$8.86^{+4.80}_{-6.49}$			$0.44^{+1.63}_{-0.21}$	0.96 (219)
HD 165024	$0.024^{+0.021}_{-0.021}$	$0.16^{+0.03}_{-0.03}$	$2.21^{+1.86}_{-0.79}$	$0.56^{+0.02}_{-0.03}$	$3.06^{+0.77}_{-0.59}$			$0.22^{+0.06}_{-0.04}$	1.07 (112)
HD 182180‡	$0.09^{+0.05}_{-0.06}$	$1.29^{+0.95}_{-0.17}$	$1.32^{+0.43}_{-0.50}$					$0.10^{+0.25}_{-0.06}$	0.86 (213)
HD 193924	$0.021^{+0.016}_{-0.016}$	$0.42^{+0.03}_{-0.02}$	$1.28^{+0.35}_{-0.26}$					$0.18^{+0.05}_{-0.04}$	1.03 (278)
HD 200775	$0.57^{+0.02}_{-0.02}$	$0.87^{+0.02}_{-0.02}$	14^{+2}_{-12}	$0.55^{+0.04}_{-0.04}$	14^{+2}_{-2}			$0.98^{+0.18}_{-0.18}$	1.88 (316)
HD 261938‡	$0.037^{+0.016}_{-0.013}$	$0.93^{+0.05}_{-0.06}$	$1.60^{+0.29}_{-0.23}$					$0.07^{+0.03}_{-0.02}$	1.02 (244)
BD-124982‡	$0.37^{+0.08}_{-0.06}$	$1.03^{+0.08}_{-0.22}$	$2.04^{+1.43}_{-0.52}$					$0.23^{+0.14}_{-0.10}$	0.99 (152)
CD-2312861‡	$0.34^{+0.01}_{-0.01}$	$3.89^{+1.38}_{-0.97}$	$3.01^{+0.70}_{-0.73}$	$0.98^{+0.02}_{-0.02}$	$18.5^{+2.0}_{-3.6}$			$0.11^{+0.03}_{-0.01}$	1.71 (452)

Names of stars are presented in Col. (1). Seven following columns consist of model parameters, and the last column contains the χ^2 value and number of degrees of freedom. The value of $N_{\rm H}^{\rm local}$ is a local hydrogen column density (see text).
† – spectra of stars could not be fitted by models with free $N_{\rm H}$, so this parameter was fixed (see text); ‡ – stars had a value $E(B-V)=0$ or were not determined in Gudennavar et al. (2012). $N_{\rm H}$ parameters are interstellar hydrogen column density.

4 ANALYSIS OF DEPENDENCIES BETWEEN X-RAYS AND STELLAR PARAMETERS

We study the possible dependencies between X-ray spectral hardness[4] and such stellar parameters as terminal velocity, mass loss rate and polar magnetic field. In addition, modeling the EPIC spectra allows us to trace the analogical dependencies for the plasma temperature and X-ray luminosity in the 0.2–8 keV range. The above mentioned dependencies can be approximated by a linear relation or by power laws

$$F(X) = A + B \cdot X, \qquad F(X) = A \cdot X^{\beta}. \qquad (5)$$

[4] See Sect. 1

Table 4 The results of fitting the correlations between L_X and stellar parameters. The proposed fit is listed in Col. (1). Col. (2) includes the correlation coefficients. Numbers of points and FAP values are written in Cols. (3) and (4) respectively. Coefficients of fits are given in Cols. (5) and (6).

Fit (1)	R (2)	N (3)	FAP (4)	A (5)	β (6)
		All OB stars			
$L_X = Av_\infty^\beta$	0.535±0.005	60	0.005	(4.88±0.61)×10^{22}	2.75±0.25
$L_X = A\dot{M}^\beta$	0.554±0.001	49	0.005	(1.95±0.13)×10^{35}	0.52±0.01
$L_X = AE_{\rm kin}^\beta$	0.772±0.002	49	0.005	(9.2±6.7)×10^{14}	0.48±0.01
		Magnetic OB stars			
$L_X = A\dot{M}^\beta$	0.717±0.02	21	0.01	(2.33±0.42)×10^{35}	0.51±0.02
$L_X = AE_{\rm kin}^\beta$	0.749±0.001	21	0.01	(5.5±4.5)×10^{14}	0.49±0.01
$L_X = A\eta^\beta$	–0.597±0.003	18	0.008	(5.78±0.53)×10^{32}	–0.43±0.02
		Nonmagnetic OB stars			
$L_X = Av_\infty^\beta$	0.706±0.005	31	0.005	(5.2±2.7)×10^{18}	4.0±0.5
$L_X = A\dot{M}^\beta$	0.768±0.002	28	0.005	(2.58±0.24)×10^{35}	0.55±0.01
$L_X = AE_{\rm kin}^\beta$	0.794±0.001	27	0.005	(5.2±4.8)×10^{14}	0.49±0.01
	OB stars with $L_X > 8\times10^{30}$ erg s^{-1} and $\eta < 5000$				
$L_X = A\eta^\beta$	–0.860±0.001	11	0.0005	(4.0±0.4)×10^{32}	–0.65±0.01

Table 5 The results of fitting the HR vs. $T_{\rm norm}$ dependence by formula $\mathrm{HR} = A + BT_{\rm norm}$ for different groups of stars enumerated in Col. (1). Cols. (2)–(3) include the correlation coefficient R and number N of objects in the group respectively. FAP values are indicated in Col. (4). Parameters of the fits are expressed in Cols. (5) and (6).

Group of stars (1)	R (2)	N (3)	FAP (4)	A (5)	B (6)
O stars	0.40±0.20	37	0.25	0.07±0.11	0.17±0.15
B stars	0.60±0.08	39	0.001	–0.02±0.11	0.39±0.15
Magnetic O stars	0.60±0.20	17	0.11	0.05±0.15	0.15±0.07
Magnetic B stars	0.65±0.11	14	0.07	0.001±0.190	0.50±0.22
Nonmagnetic O stars	0.50±0.34	20	0.4	0.06±0.11	0.07±0.42
Nonmagnetic B stars	0.45±0.06	25	0.05	–0.03±0.10	0.39±0.19

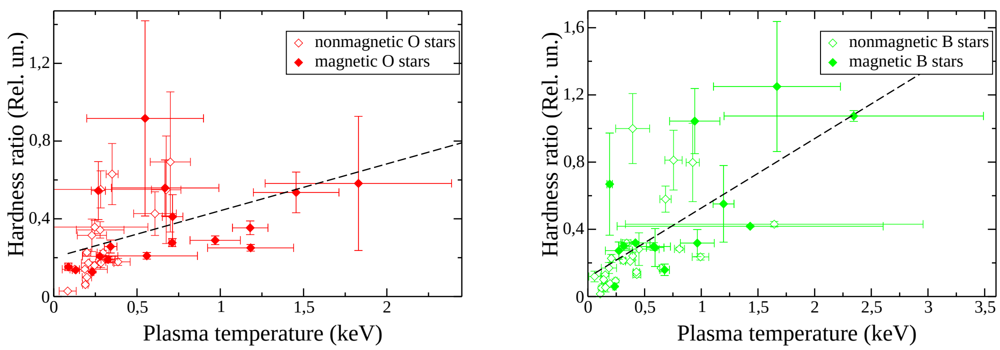

Fig. 2 The correlations between spectral hardness and plasma temperature for O stars (*left panel*) and for B stars (*right panel*). The linear fit for all considered OB stars is signified by *dotted lines*.

Here X is one of the examined stellar parameters. To find the coefficients of the fit for Equation (5), we performed a usual regression analysis of the proposed correlation for all objects in our sample, both for magnetic and for nonmagnetic OB stars (e.g., Taylor 1982). For each of the proposed dependences, the correlation coefficient R was evaluated. False Alarm Probability (FAP) values corresponding to the obtained correlation coefficient were estimated accordingly by Taylor (1982).

The estimation of correlation coefficients and FAP values indicates that not all of the expected correlations take place. We find that real dependencies exist between X-ray luminosity L_X and mass loss rate $\dot{M}$, kinetic energy of stellar wind $E_{\rm kin}$ and magnetic confinement parameter η. The

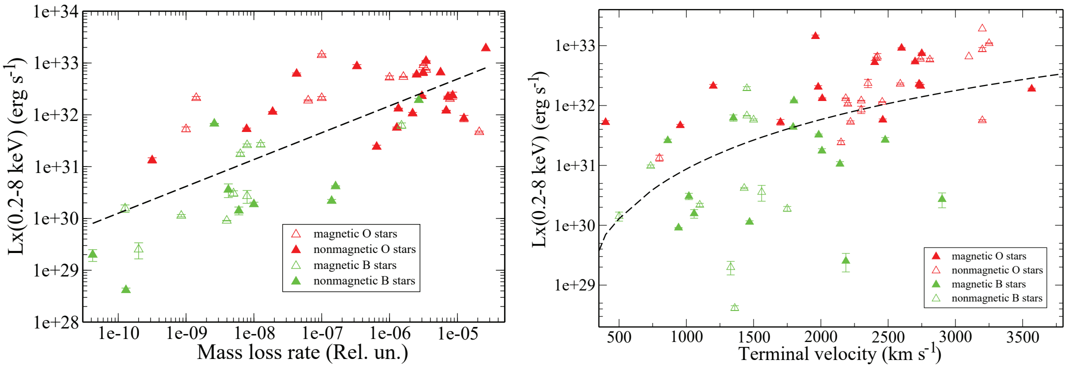

Fig. 3 The correlations between stellar X-ray luminosity and mass loss rate (*left panel*) and terminal wind velocity (*right panel*). The mass loss rates are presented in solar mass per year. The fits for all our sample of OB stars are signified by *dotted lines*.

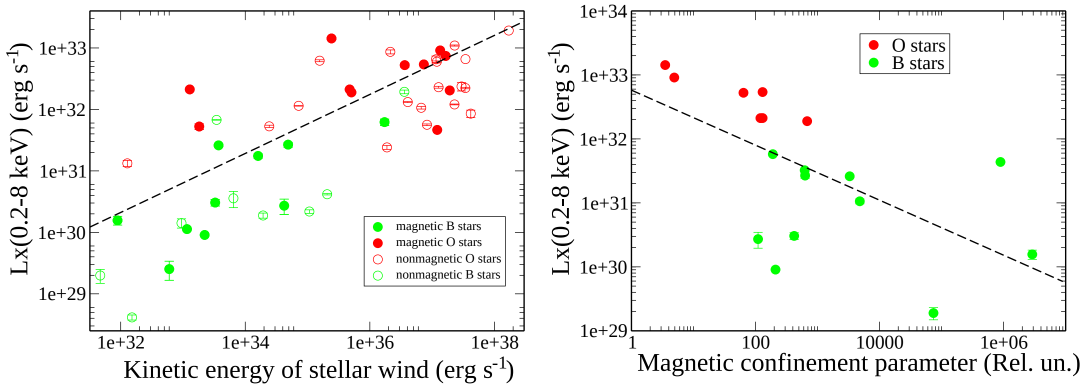

Fig. 4 The correlations between stellar X-ray luminosity and kinetic energy of stellar wind (*left panel*) and magnetic confinement parameter η (*right panel*). *Dotted lines* indicate the power fits of studied dependencies.

last one is determined by Equation (6) in Ud-Doula et al. (2008)

$$\eta = \frac{B_p^2 R_*}{4\dot{M} v_\infty}\,, \qquad (6)$$

where B_p is the polar magnetic field, R_* is the stellar radius, $\dot{M}$ is the mass loss rate and v_∞ is the wind's terminal velocity.

In the present paper, we take η values reported by Petit et al. (2013). The R and FAP values calculated by us and also the approximate coefficients are presented in Table 4.

A special case is represented by the dependence between the spectral hardness HR and averaged plasma temperature $T_{\rm norm}$. In the case of purely thermal plasma, these dependencies have to be linear. Real dependencies are plotted in the panels of Figure 2. The corresponding correlation coefficients R and FAP for different groups of OB stars are expressed in Table 5. As is well known, the correlation is only real in the case of FAP< 0.01. This means that HR only linearly depends on $T_{\rm norm}$ for B stars. For other types of OB stars, the spectral hardness increases with plasma temperature but the real dependence differs from a linear one.

It can definitely mean that there is an additional (probably non-thermal) contribution to X-ray emission of OB stars.

According to estimations by Babel & Montmerle (1997), the X-ray luminosity is determined by stellar parameters via the following expression

$$L_{\rm X} = 2.6{\times}10^{32}\,\dot{M}_{10}\left(\frac{v_\infty}{10^3\ {\rm km\,s^{-1}}}\right) B_{\rm kG}^{0.4}\,{\rm erg\,s^{-1}}, \qquad (7)$$

where $\dot{M}_{10}$ is mass loss rate in units of $10^{-10} M_\odot\,{\rm yr}^{-1}$, $B_{\rm kG}$ is polar magnetic field given in kG and terminal velocity v_∞ is expressed in $10^3\,{\rm km\,s^{-1}}$. It means that L_X should depend linearly on terminal wind velocity and mass loss rate. The dependence on the magnetic field can be described by a power law.

Our analysis (see Table 4) demonstrates the power dependence of L_X on mass loss rate, terminal wind velocity, kinetic energy of stellar wind and magnetic confinement parameter η. The corresponding fits are depicted in Figures 3–4. Power dependence of X-ray luminosity on mass loss rate was also reported by Nazé et al. (2014). Their fit is similar to ours, but unlike us these authors only analyzed stars with measured magnetic fields.

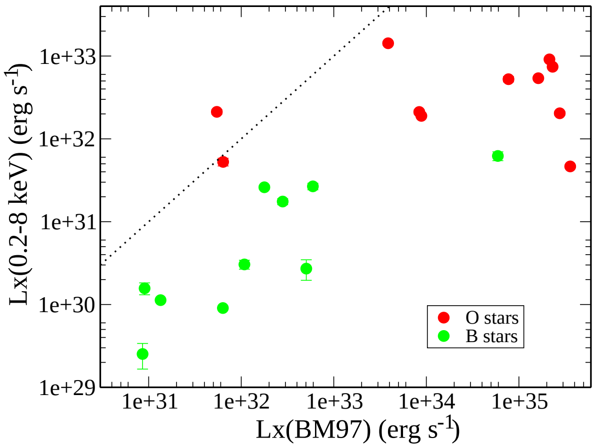

Fig. 5 Comparison of the X-ray luminosities of OB stars with the predicted values applying the expression of Babel & Montmerle (1997).

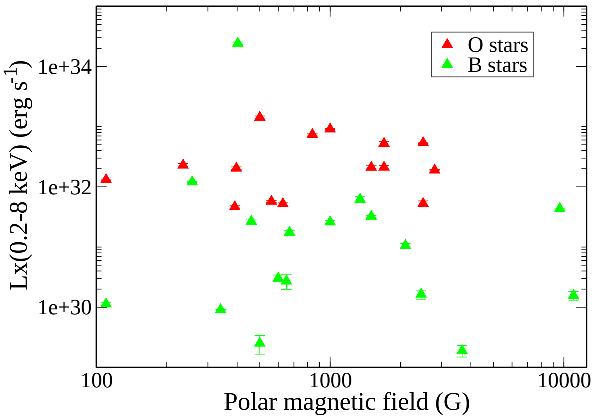

Fig. 6 The dependence between observational X-ray luminosity of OB stars and their magnetic fields.

In addition, we compare model X-ray luminosity calculated employing Equation (7) from that obtained with our analysis of *XMM-Newton* observations of magnetic OB stars. As we can see in Figure 5, the model L_X luminosities in most cases are one-two orders higher than those obtained from observations. This discrepancy is also mentioned by ud-Doula et al. (2014) and Nazé et al. (2014). The last authors connected this discrepancy with an uncertain bandpass used by Babel & Montmerle (1997) for their estimations.

However, in the present paper the dependencies of L_X on the stellar parameters, both for all examined OB stars and separately for nonmagnetic stars, are studied. Our analysis shows that dependencies of X-ray luminosity for OB stars with weak magnetic field are similar to those for magnetic OB stars. Moreover, there are no correlations of $L_{\rm X}$ values with the polar magnetic field of the stars, as seen in Figure 6.

Surprisingly, we detected the correlation of X-ray luminosity with the magnetic confinement parameter η. We ascertain in Figure 4 that the power of X-ray luminosity decreases with growing η. This dependence is better expressed for stars with $L_{\rm X} > 8{\times}10^{30}\,{\rm erg\,s^{-1}}$ and confinement parameter $\eta < 5000$.

Inspecting Equation (5), we see that the confinement parameter η is inversely proportional to the mass loss rate and terminal wind velocity. We can explain the decreasing X-ray luminosity with the magnetic confinement parameter η by taking into account this proportionality and dependencies of the L_X values on $\dot{M}$ and v_∞ presented in Table 4. As we mention above, there is no clear evidence that X-ray luminosity $L_{\rm X}$ depends on the stellar magnetic field. It can mean that the proportionality of the parameter η to the square of the surface magnetic field strength leads mainly to scattering of the points in Figure 4.

Resuming, we can conclude that X-ray luminosity can be approximated by the following relations

$$L_{\rm X} \approx 9.2{\times}10^{14} E_{\rm kin}^{0.5}, \quad \text{and} \quad L_{\rm X} \approx 9.2{\times}10^{14} \dot{M}_{10}^{0.5} v_\infty, \tag{8}$$

where $\dot{M}$ and v_∞ are given in units of $10^{-10}\,M_\odot\,{\rm yr}^{-1}$ and in ${\rm km\,s^{-1}}$ respectively.

5 GENERAL CONCLUSIONS

The goal of the present paper is studying the X-ray emission of OB stars, both magnetic and non-magnetic stars. We have analyzed the X-ray spectra of 93 OB stars. Spectra were extracted and fitted by thermal models by taking into account both interstellar and local absorption. The correlations between spectral hardness and average plasma temperature with polar magnetic field B, mass loss rate $\dot{M}$ and wind terminal velocity V_∞ were examined.

The result of our analysis can be summarized in the following conclusions:

– The X-ray luminosity for all kinds of OB stars strongly increases with growing terminal wind velocity.
– The X-ray luminosity of OB stars $L_{\rm X} \propto \dot{M}^{0.5}$ and $L_{\rm X} \propto E_{\rm kin}^{0.5}$ for both O and B stars.
– Analyzing the correlations between X-ray hardness and average plasma temperature provides evidence that there can be an additional mechanism for generation of non-thermal X-rays for at least some studied OB stars.
– There are no significant differences in the properties of X-ray emission for both magnetic and non-magnetic OB stars.

Acknowledgements AK is grateful for support from the Russian Science Foundation grant (No. 18–12–00423).

References

Alecian, E., Kochukhov, O., Neiner, C., et al. 2011, A&A, 536, L6
Alecian, E., Kochukhov, O., Petit, V., et al. 2014, A&A, 567, A28
Anders, E., & Grevesse, N. 1989, Geochim. Cosmochim. Acta, 53, 197
Babel, J., & Montmerle, T. 1997, A&A, 323, 121
Bertout, C., Leitherer, C., Stahl, O., et al. 1985, A&A, 144, 87
Bouret, J. C., Hillier, D. J., Lanz, T., & Fullerton, A. W. 2012, A&A, 544, A67
Cohen, D. H., Cassinelli, J. P., & MacFarlane, J. J. 1997, ApJ, 487, 867
Cohen, D. H., Kuhn, M. A., Gagné, M., Jensen, E. L. N., & Miller, N. A. 2008, MNRAS, 386, 1855
De Becker, M., del Valle, M. V., Romero, G. E., Peri, C. S., & Benaglia, P. 2017, MNRAS, 471, 4452
Drew, J. E., Denby, M., & Hoare, M. G. 1994, MNRAS, 266, 917
Fierro-Santillán, C. R., Zsargó, J., Klapp, J., et al. 2018, ApJS, 236, 38
Fossati, L., Castro, N., Morel, T., et al. 2015, A&A, 574, A20
Gagné, M., Fehon, G., Savoy, M. R., et al. 2011, ApJS, 194, 5
Garcia, M., & Bianchi, L. 2004, ApJ, 606, 497
Grunhut, J. H., Wade, G. A., Marcolino, W. L. F., et al. 2009, MNRAS, 400, L94
Gudennavar, S. B., Bubbly, S. G., Preethi, K., & Murthy, J. 2012, ApJS, 199, 8
Howarth, I. D., Siebert, K. W., Hussain, G. A. J., & Prinja, R. K. 1997, MNRAS, 284, 265
Hubrig, S., Schöller, M., Kharchenko, N. V., et al. 2011, A&A, 528, A151
Hubrig, S., Schöller, M., Ilyin, I., et al. 2013, A&A, 551, A33
Kurapati, S., Chandra, P., Wade, G., et al. 2017, MNRAS, 465, 2160
Lamers, H. J. G. L. M., Haser, S., de Koter, A., & Leitherer, C. 1999, ApJ, 516, 872
Liedahl, D. A., Osterheld, A. L., & Goldstein, W. H. 1995, ApJL, 438, L115
Markova, N., Puls, J., Repolust, T., & Markov, H. 2004, A&A, 413, 693
Markova, N., Puls, J., Scuderi, S., & Markov, H. 2005, A&A, 440, 1133
Martins, F., Schaerer, D., Hillier, D. J., et al. 2005, A&A, 441, 735
Martins, F., Donati, J. F., Marcolino, W. L. F., et al. 2010, MNRAS, 407, 1423
Mewe, R., Gronenschild, E. H. B. M., & van den Oord, G. H. J. 1985, A&AS, 62, 197
Mewe, R., Lemen, J. R., & van den Oord, G. H. J. 1986, A&AS, 65, 511
Morrison, R., & McCammon, D. 1983, ApJ, 270, 119
Najarro, F., Hanson, M. M., & Puls, J. 2011, A&A, 535, A32
Nazé, Y., Walborn, N. R., Rauw, G., et al. 2008, AJ, 135, 1946
Nazé, Y., Petit, V., Rinbrand, M., et al. 2014, ApJS, 215, 10
Nazé, Y., Gosset, E., Mahy, L., & Parkin, E. R. 2017, A&A, 607, A97
Perryman, M. A. C., Lindegren, L., Kovalevsky, J., et al. 1997, A&A, 500, 501
Petit, V., Owocki, S. P., Wade, G. A., et al. 2013, MNRAS, 429, 398
Pillitteri, I., Fossati, L., Castro Rodriguez, N., Oskinova, L., & Wolk, S. J. 2018, A&A, 610, L3
Pollock, A. M. T. 2007, A&A, 463, 1111
Prinja, R. K., Stahl, O., Kaufer, A., et al. 2001, A&A, 367, 891
Rauw, G., Blomme, R., Waldron, W. L., et al. 2002, A&A, 394, 993
Repolust, T., Puls, J., & Herrero, A. 2004, A&A, 415, 349
Ryspaeva, E., & Kholtygin, A. 2018, RAA (Research in Astronomy and Astrophysics), 18, 104
Ryspaeva, E., & Kholtygin, A. 2019, RAA (Research in Astronomy and Astrophysics), 19, 120
Sana, H., Stevens, I. R., Gosset, E., Rauw, G., & Vreux, J. M. 2004, MNRAS, 350, 809
Shenar, T., Oskinova, L. M., Järvinen, S. P., et al. 2017, A&A, 606, A91
Smith, R. K., Brickhouse, N. S., Liedahl, D. A., & Raymond, J. C. 2001, ApJL, 556, L91
Sundqvist, J. O., ud-Doula, A., Owocki, S. P., et al. 2012, MNRAS, 423, L21
Taylor, J. R. 1982, An Introduction to Error Analysis, The Study of Uncertainties in Physical Measurements (Oxford: University Press, and Mill Valley: University Science Books)
ud-Doula, A., & Owocki, S. P. 2002, ApJ, 576, 413
Ud-Doula, A., Owocki, S. P., & Townsend, R. H. D. 2008, MNRAS, 385, 97
ud-Doula, A., Owocki, S., Townsend, R., Petit, V., & Cohen, D. 2014, MNRAS, 441, 3600
van Leeuwen, F. 2007, A&A, 474, 653
Vink, J. S., Davies, B., Harries, T. J., Oudmaijer, R. D., & Walborn, N. R. 2009, A&A, 505, 743
Wade, G. A., Barbá, R. H., Grunhut, J., et al. 2015, MNRAS, 447, 2551
Wilms, J., Allen, A., & McCray, R. 2000, ApJ, 542, 914